2Kx2K molecular beam epitaxy HgCdTe detectors for the James Webb Space Telescope NIRCam instrument

J.D. Garnett*, M. Farris, S. Wong, M. Zandian, Rockwell Scientific Company
D.N.B. Hall, S. Jacobson, G. Luppino, S. Parker, Institute for Astronomy, University of Hawaii
D. Dorn, S. Franka, E. Freymiller, S. McMuldroch, Ball Aerospace & Technologies Corporation

ABSTRACT

The NIRCam instrument will fly ten of Rockwell Scientific's infrared molecular beam epitaxy HgCdTe 2048x2048 element detector arrays, each the largest available with current technology, for a total of 40 Megapixels. The instrument will have two varieties of MBE HgCdTe, a SWIR detector with λ_{co} = 2.5 μm, for the shortwave channel of NIRCam (0.6-2.3 μm); and a MWIR detector with λ_{co} = 5.3 μm, for the longwave channel of NIRCam (2.4-5.0 μm). Demonstrated mean detector dark currents less than 0.01 electrons per second per pixel at operating temperatures below 42 K for the MWIR and below 80 K for the SWIR, combined with quantum efficiency in excess of 80 percent and read noise below 6 electrons rms, make these detector arrays by far the most sensitive SWIR and MWIR devices in the world today. The unique advantages of molecular beam epitaxy as well as FPA data on noise, dark current, quantum efficiency, and other performance metrics will be discussed. In addition, the focal plane assembly package designs will be presented and discussed.

Keywords: James Webb Space Telescope (JWST), Near Infrared Camera (NIRCam), Sensor Chip Assembly (SCA), Focal Plane Assembly (FPA), Molecular beam epitaxy (MBE), HgCdTe, SWIR, MWIR

1. INTRODUCTION

The James Webb Space Telescope (JWST) is the premiere space telescope for the second decade of the new millennium. The core imager instrument on the telescope will be the Near Infrared Camera (NIRCam), which will contain a 40-million-pixel focal plane. This focal plane will consist of two identical branches, each of which contains a 2x2 focal plane assembly (FPA) mosaic of 2048x2048 detector arrays covering the wavelength range from 0.6 μm – 2.4 μm; and a single FPA 2048x2048 detector array covering the wavelength range from 2.5 μm – 5.0 μm.

The detectors chosen to populate the NIRCam instrument are Rockwell Scientific's molecular beam epitaxy (MBE) HgCdTe infrared arrays. For the shortwave arm of the instrument (0.6 μm – 2.5 μm), RSC will provide substrate removed, λ_{co} ~ 2.5 μm MBE HgCdTe material, denoted "VIS/SWIR". For the longwave arm of the instrument (2.5 μm – 5.0 μm), RSC will provide λ_{co} ~ 5.3 μm MBE HgCdTe material, denoted "MWIR."

The remarkable performance of these MBE HgCdTe detector arrays will benefit tremendously the NIRCam instrument in its exploration of the universe's first light and in its study of the early period of galaxy assembly, stars and stellar systems; and its search for planetary systems and the conditions for life.

2. MBE HgCdTe 2Kx2K DETECTOR ARRAYS

NASA's JWST Packaging and Manufacturing Technology (PMT) development program that ran from 2000–2003 provided the vehicle for Rockwell Scientific to demonstrate that large-format, MBE "bandgap engineered", double layer planar heterostructure (DLPH) architecture detector arrays [1] could meet and often exceed the JWST detector performance specifications. The program also produced the 2048x2048 readout integrated circuit, the HAWAII-2RG [2], for hybridization to our MBE HgCdTe detector material. This readout meets and often exceeds JWST multiplexer requirements and is now in full production for both JWST and ground-based astronomy applications.

We show below the growth and process techniques for the detector arrays produced under the PMT program, hybridized to the JWST HAWAII-2RG readout integrated circuit (H-2RG ROIC), result in mean dark currents below 0.005 e-/sec for MWIR material from 30 K to 45 K and for VIS/SWIR material from 30 K to 80 K; total 1,000 second integrated

*Further author information: jgarnett@rwsc.com

noise below 9 e-rms (Fowler-8 sampling); quantum efficiencies after antireflection coating above 80% over the entire wavelength range from visible to 5µm and in excess of 90-95% over select regions of the wavelength range; nearest neighbor cross talk below 2%; and latent images below 0.03% of the source fluence. We call the detector array hybridized to the H-2RG ROIC and mounted to its carrier package the Sensor Chip Assembly or SCA.

2.1 Dark current and total integrated noise

Rockwell Scientific Company (RSC) has demonstrated performance on sample 2K x 2K devices that exceeds the NIRCam dark current requirement of less than 0.01 e-/sec in a 1,000 second integration time and with substantial margin in operating temperature. The dark current data shown in Figure 1 are for substrate-thinned (H2RG-5.2µm-015) and substrate-removed (H2RG-5.3µm-006) MWIR material. The nomenclature for a particular device is denoted "H2RG-x.xµm -yyy", where "H2RG" denotes the H-2RG ROIC, "x.xµm" denotes the cut-off wavelength x.x at 37 K in units of microns, and "yyy" denotes the particular hybridization number in the production sequence.

RSC's MWIR MBE HgCdTe detectors exhibit dark currents in the range 0.001 to 0.01 e-/sec, as shown in Figure 1. These are relatively insensitive over the temperature range from 30 to 45 K. The dark current floor is approximately 0.0025 e-/sec for H2RG-5.3µm-006 and 0.004 e-/sec for H2RG-5.2µm-015. At higher temperatures, the theoretical-limiting diffusion dark current becomes dominant. It dominates for temperatures above ~ 50 K and increases about an order of magnitude for each 10 K increment in temperature. The only temperature-dependent performance characteristic over the 30 to 45 K temperature range is a very slight increase in the few percent of pixels exceeding set dark current clips of 0.01, 0.02, and 0.05 e-/sec used for analysis of our data.

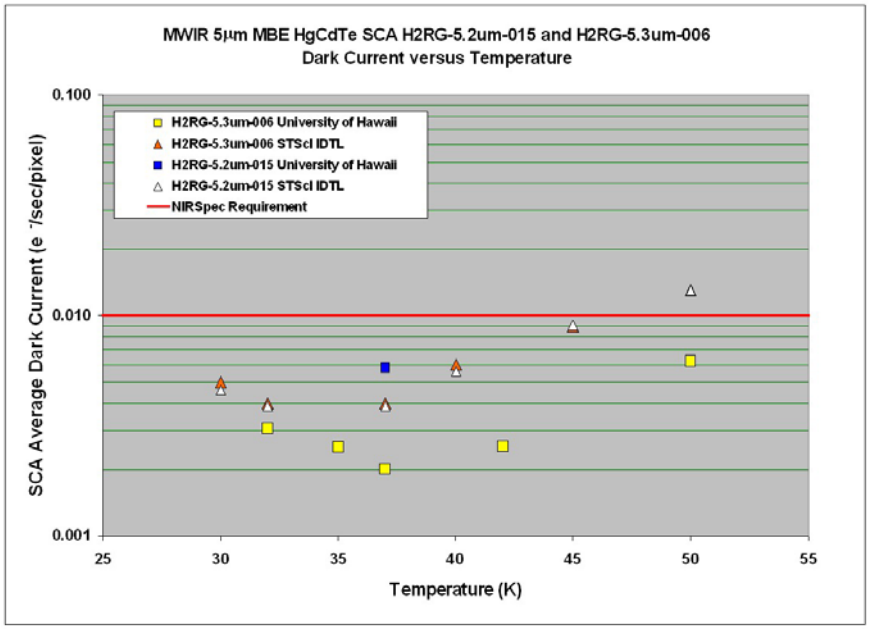

Figure 1. MWIR MBE HgCdTe dark current vs. temperature — performance exceeds the NIRCam requirement for MWIR SCAs from the JWST PMT program in over 95% of the pixels for H2RG-5.3µm-006 and 75% for H2RG-5.2µm-015 (85% of the pixels are below 0.05 e-/sec). Some of the data are provided courtesy of Dr. Don Figer, the Independent Test Lab (IDTL) at Space Telescope and Science Institute (STScI).

The very low dark current, which remains flat over a wide temperature range, translates into a higher temperature of operation at which the detector array can still meet the dark current requirement. The significant operating temperature margin translates into system level advantages in weight, power and thermal tolerance during flight. It provides tolerance to temperature drifts in the NIRCam instrument as well as increased reliability for the life of the mission if the system must operate warmer than planned.

Although the 0.6 – 2.4 µm SWIR detectors were not included in NASA's PMT program, the RSC team characterized two 2.5 µm MBE HgCdTe detectors recently produced for ground-based astronomy programs. These SCAs use the

same H-2RG ROIC as JWST, a nearly identical package to that proposed by RSC for NIRCam, and the same MBE material process. They are identical to the MWIR SCAs except for the cut-off wavelength and the fact that the material growth was not optimized for JWST backgrounds and temperatures. These SWIR detectors exhibit low dark current performance with floor values very comparable to the best MWIR material; H2RG-2.5µm-011 has dark current between 0.002 and 0.003 e-/sec over the 30 to 45 K temperature range. Furthermore, in the SWIR detectors, the onset of diffusion current is delayed to ~ 80 K as predicted by scaling of the theoretical diffusion current with bandgap energy. As shown in Figure 2, H2RG-2.5µm-011 has dark current ~ 0.007 e-/sec at 80K. This performance was achieved in spite of these detectors being optimized for a much higher operating temperature.

Most of the dark current data is for a detector applied reverse bias of –250 mV, corresponding to well depth > 84,000 e- for a node capacitance of ~ 45 fF and a pedestal injection of approximately –50 mV, which results in a true detector reverse bias of –300 mV after release of the reset. The JWST-required minimum full well is 60,000 e-.

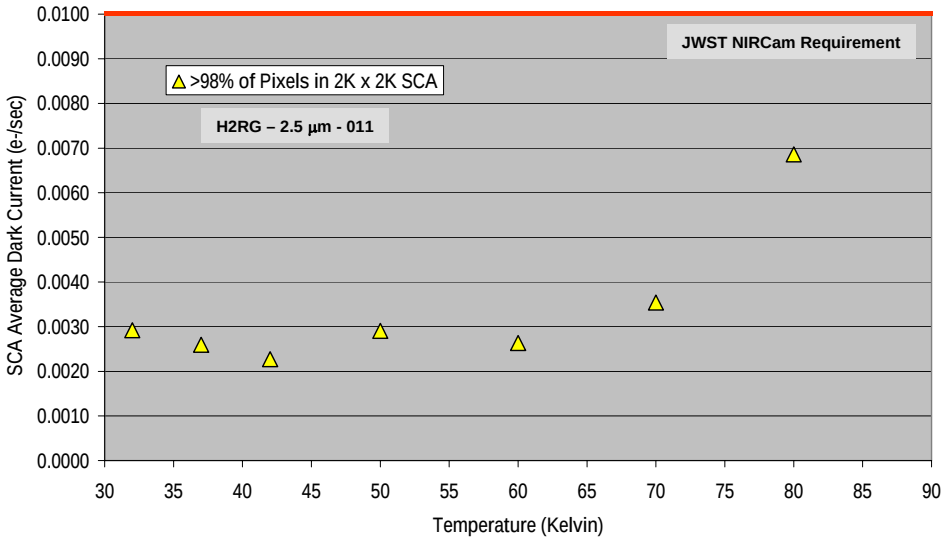

Figure 2. SWIR MBE HgCdTe dark current versus temperature — performance exceeds the NIRCam requirement in over 98% of the pixels.

The dark currents shown above are determined from standard test sequences consisting of five identical ramps, each involving a pixel-by-pixel reset sequence, followed by 145 frames sampled up-the-ramp at 12-second intervals over a total of 1,740 seconds. The dark current is determined for the four separate 1 Megapixel vertical "stripes" of the SCA using the horizontal reference pixels at the top and bottom of the stripes to correct for DC drifts [2]. For these detectors, even after 1,000 seconds, the typical 2 – 4 e- accumulated charge due to dark current is a small fraction of the single CDS read noise and still below even the 16-16 CDS (Fowler-16) read noise of ~ 4 e- rms. We accordingly use a 16-16 CDS frame over a 1,536-sec interval to derive dark current histograms for the five individual ramps.

Although "glow" (charge per read) is not explicitly referenced in the JWST requirements documents, our dark current data allows us to set a stringent upper limit of < 0.02 e-/read on "glow" effects. This level is low enough to allow complete sampling flexibility in NIRCam observing sequences.

The NIRCam requirement for total integrated noise (includes dark current noise, readout noise, and any additional 1/f drift noise contributions) is less than 9 e-rms in a 1,000 second integration using Fowler-8 sampling. RSC has demonstrated noise performance better than 8 e-rms (Fowler-8) over the temperature range 30 to 50 K for the MWIR arrays and over 30 to 80 K for the SWIR arrays (Figure 3).

To obtain accurate per pixel dark current and total noise histograms over the entire 2Kx2K array, we conducted a limited number of tests involving 32 ramps, each of 145 frames following two pixel-by-pixel resets, a total integration time of 58,000 seconds. Data storage limitations allowed only the first nine frames, eight at approximately 1,000 seconds (864 seconds); and the final eight frames (at 1632 seconds) to be written to disk. CDS frames formed by

subtracting the initial frames from the 864 second frames are used to generate the 32 ramps x 2048 x 2048 pixel cubes for 1, 2, 4, and 8 averages (the highest point in each pixel string is discarded to eliminate cosmic ray effects). The mean of each pixel string estimates the dark current and the data are clipped at a 0.025 e-/sec value. The standard deviation of each remaining pixel string estimates the total noise in an 864-second exposure. The same procedure is used for the 1632 second frames and also for the CDS 1632 – 864 frames. Adjacent ramps are averaged to simulate 16 and 32 averaged total noise from the existing data. Examples of the dark current and 32 averaged standard deviation histograms sampling up the ramp are shown in Figures 4 and 5.

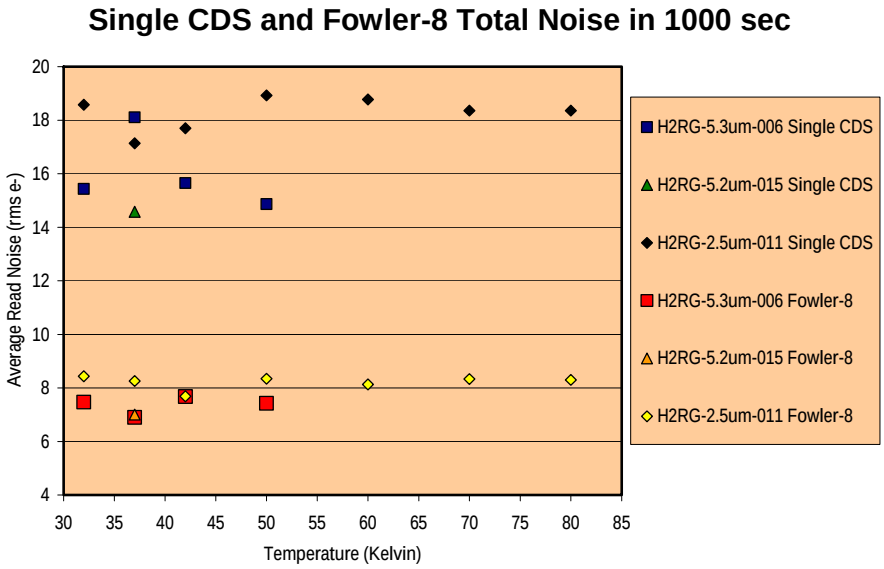

Figure 3. CDS and Fowler-8 total read noise in 1,000 seconds versus temperature.

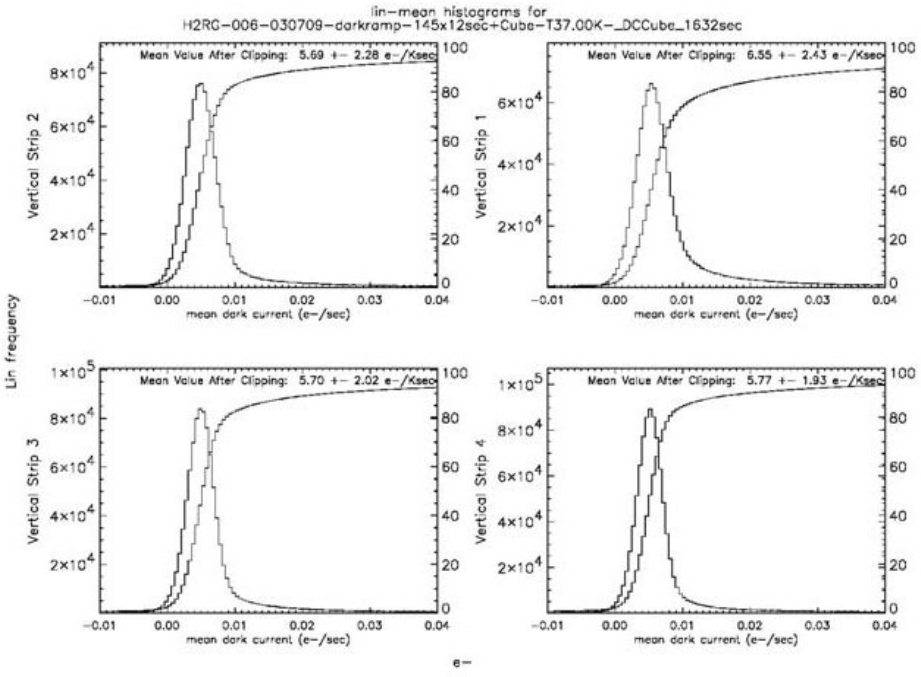

Figure 4. Dark current histograms for H2RG-5.3um-006. Plots are of each of the 1 Mexapixel outputs of the H-2RG and represent a mean dark current less than 0.006 e-/second. The histograms are derived from 32 half-hour ramps — the technique of obtaining these data is described in the text.

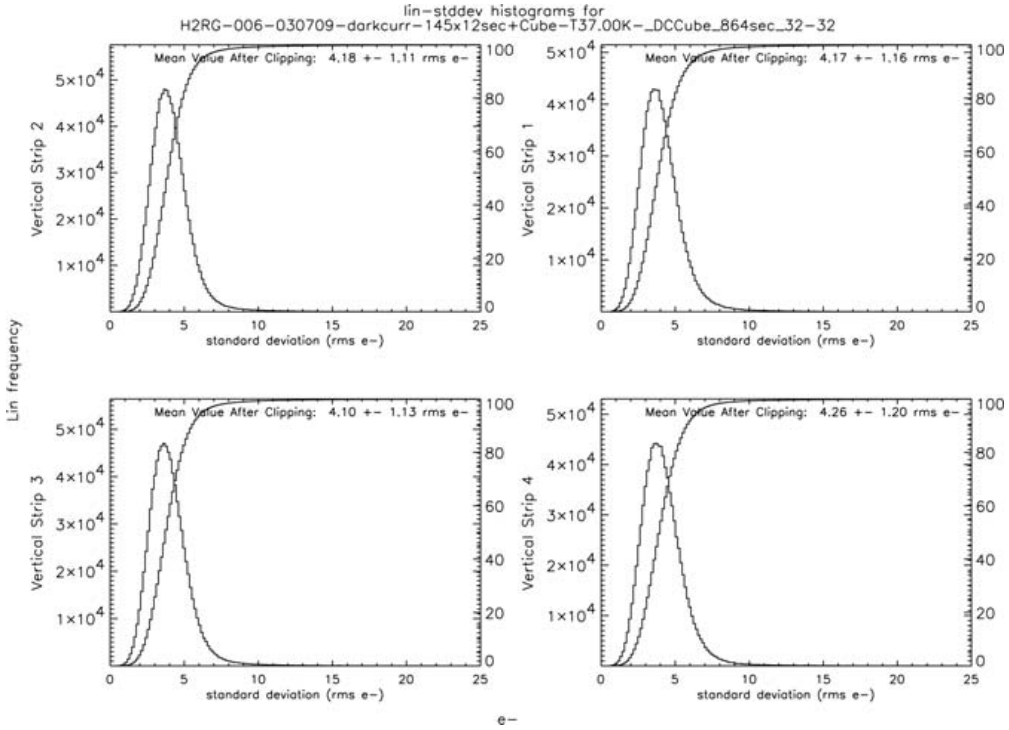

Figure 5. Total 864 second 32-32 averaged CDS (Fowler-32) noise derived from the standard deviation among 32 independent ramps of data. Plots are of each of the 1 Megapixel outputs of the H-2RG and represent the total noise in an 864 second exposure. The technique for obtaining these data is described in the text.

2.2 Detective quantum efficiency (DQE)

The NIRCam requirement specifies greater than 70% DQE for wavelengths between 0.6 and 1.0 µm, and greater than 80% DQE for wavelengths between 1.0 and 5.0 µm. RSC has demonstrated performance that exceeds 80% at all wavelengths, with greater than 90% achieved in over half of the long wavelength band specified.

Figure 6 shows a grayscale map of H2RG-5.2µm-015 with good uniformity across the array. These data were taken in the astronomy K-Band (2.0 to2.4 µm) at 37 K. The histogram of the same array (Figure 7) shows the tight distribution with peak DQE at 95%. This performance meets both the JWST requirement and goal. The inset in Figure 6 shows the average DQE (96.8%) and operability (99%) obtained for a million element quadrant (1025 x 1025) centered in the bottom half of the array. This demonstrates the excellent DQE and uniformity that can be anticipated with the improvements that naturally occur with larger numbers of production lots compared to the limited lot runs under the JWST PMT program.

For detailed spectral measurements of the DQE, we use process evaluation chips or PECs. PECs are processed on the same CdZnTe/HgCdTe detector layers as the 2Kx2K detector arrays and are diced out at completion of detector layer processing to evaluate the final quality of the detector array material. To evaluate the spectral response for substrate-removed detectors, these PECs were diced out and then flip-chip hybridized to a fanout. They then underwent the same substrate removal and antireflection coating process as the SCAs.

Figure 8 shows the DQE spectral response obtained on a VIS/SWIR PEC hybrid taken from the same layer as H2RG-2.5µm-011. The data shows excellent flat DQE response from the visible to the SWIR cutoff wavelength, 600 nm – 2500 nm. (This detector material was not optimized for the NIRCam operation temperature range.) Theoretical curves both for the present layer and for a layer optimized for NIRCam (lower doping) provide good evidence that we will be able to adjust the doping and exceed the NIRCam DQE requirements for our VIS/SWIR detector material.

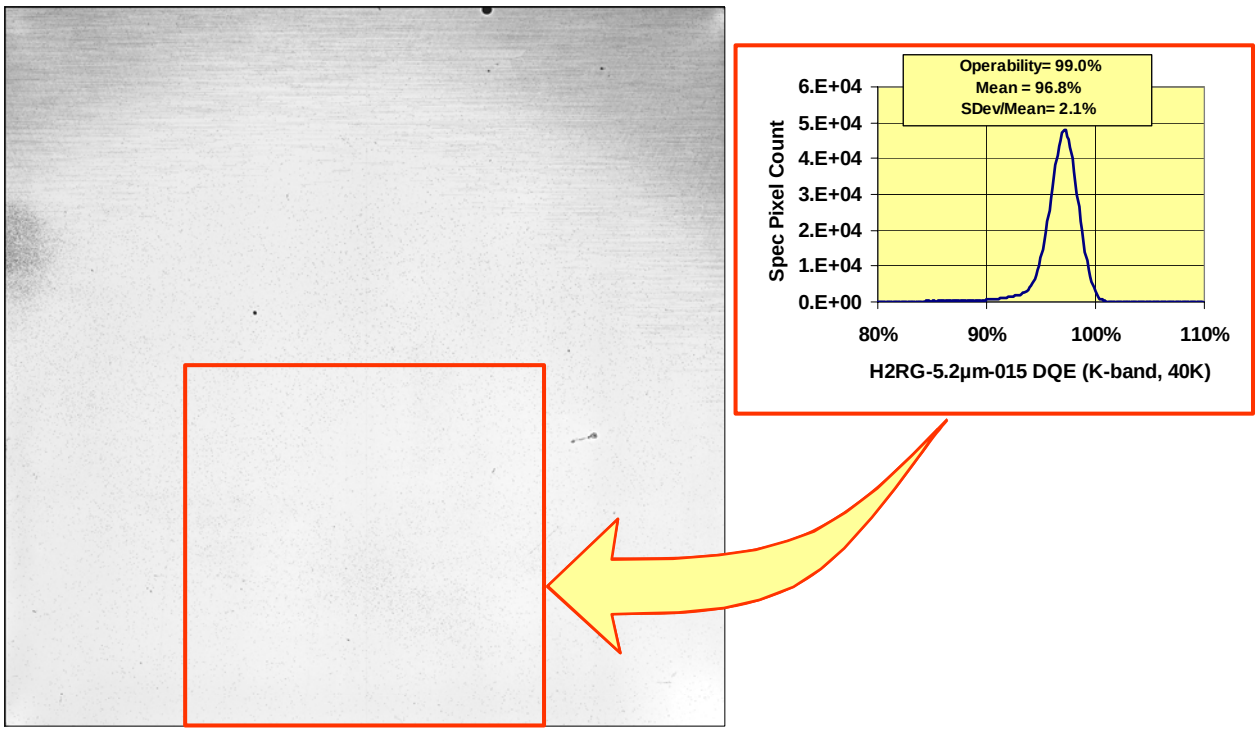

Figure 6. DQE grayscale of H2RG-5.2um-015 shows good uniformity and few clusters of bad pixels. The solid dark band around the periphery of the array is the embedded reference pixels. The shaded pixels near the top corners of the array are lower response pixels due to a processing mistake. The inset demonstrates mean DQE = 96.8%, operability >99%, and sigma/mean = 2.1%.

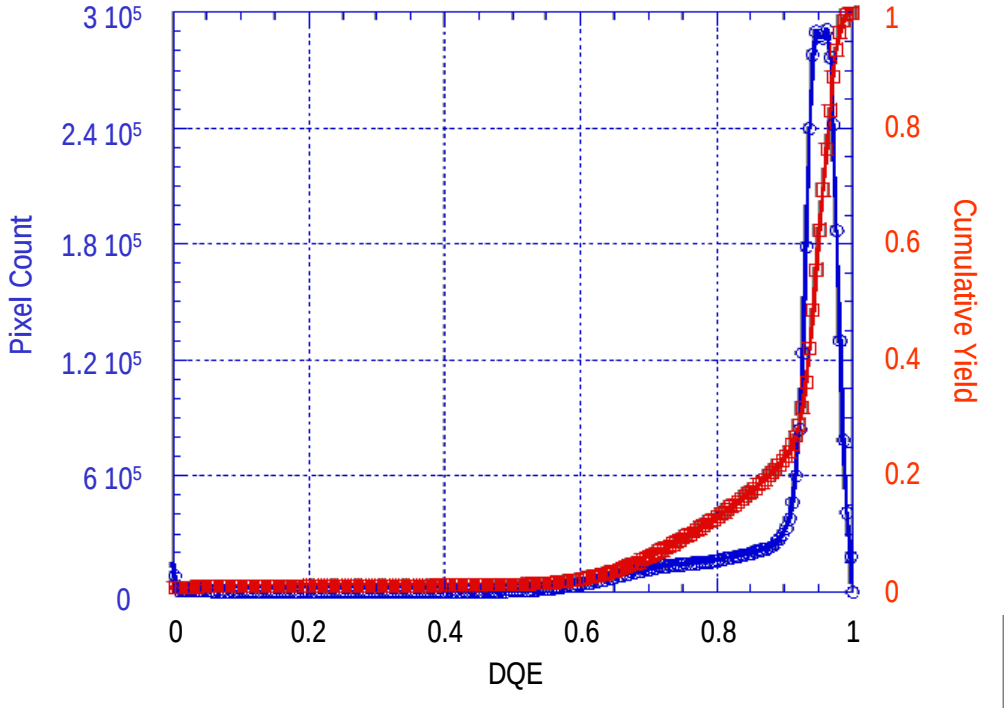

Figure 7. DQE histogram for the entire SCA — shows a strong peak at 0.95, with the main population tightly distributed about the mean.

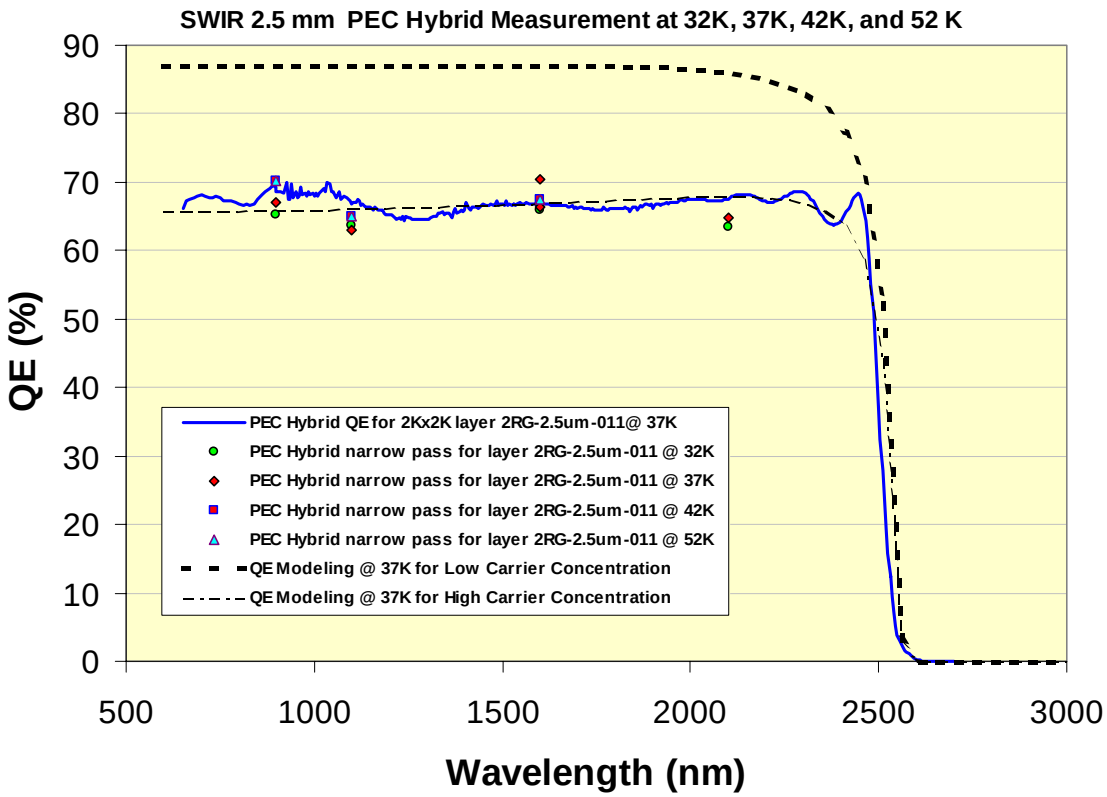

Figure 8. Spectral QE measurements from a substrate-removed SWIR PEC hybrid — show flat response across the entire region from 0.6 to 2.5 microns. This layer has not been optimized for carrier concentration for the NIRCam temperature requirements. Theoretical curves for the present and predicted improved performance are shown.

2.3 Cross talk

When cosmic rays pass through the detector material, numerous charge pairs are created along the path of the particle. This event deposits signal in a much tighter spatial pattern than could be created optically. If we choose events in which the cosmic ray passes through the center of the pixel, signals in the surrounding pixels provide a good measure of the cross talk.

We used cosmic ray hits in 1,740 second dark ramp exposures to measure the cross talk. These experiments were performed with a 2.5µm cutoff SCA, not substrate-removed, operating at 37 K. Since the cosmic ray deposits a line of ionized charge as it passes through the pixel, the detector cutoff is irrelevant. In these dark frames and the histograms, cosmic ray events show up prominently. Their frequency falls off inversely with the count induced, with events above 8,000 ADU extremely rare. We bin these events into induced count bins and then screen to retain only those events where the four adjacent row/column pixel signals agree within some criterion — usually a factor of four. This criterion selects events in which the cosmic ray passes through very near the center of a pixel, producing balanced signals in adjacent pixels. The signals for the eight adjacent "tic-tac-toe" pixels are then each normalized to that of the central pixel. A suitable median averaging is then used to derive the charge cross talk. In practice, the charge estimates are relatively insensitive to the value and a 25% median appears optimum.

Typical data for 189 events with charge in the 4,000 – 12,000 e- range are shown in Figure 9. Cross talk analysis by cosmic ray hit data taken at 42 K shows essentially identical results as those presented above; i.e., we find a nearest neighbor cross talk below about 1.4% and indistinguishable from the noise in the corner neighbors. Nearly identical results were obtained by Dr. Don Figer at the Independent Test Lab (STScI) using the 5.2µm cutoff SCA H2RG-5.2µm-015.

These cross talk values exceed the NIRCam requirement of 5% and even exceed the 2% goal.

0.03%	1.32%	0.03%
1.40%	100%	1.42%
0.01%	1.26	0.00%

Figure 9. Cosmic ray induced cross talk in H2RG-2.5µm-011 at 37K — for 189 primary events in the 4,000 – 12,000 e- range.

2.4 Latent image

The NIRCam requirment specifies less than 0.1% (0.01% goal) after the second read following an exposure of > 80% of full well. RSC's MBE HgCdTe devices operate near the goal level.

RSC's lattice matched MBE HgCdTe on CdZnTe substrates is characterized by extremely low image persistence after two frame resets. This persistence can be characterized as a decaying dark current or as a total persistence charge released after specified intervals.

The latent image of the H-2RG MBE SCA dies off very rapidly with resets after an initial exposure near full well. Figure 10 shows a typical latent image for full well source exposure. All latent images, versus wavelength of source and magnitude of the exposure (up to 1000 percent full well) easily exceed the NIRCam requirement.

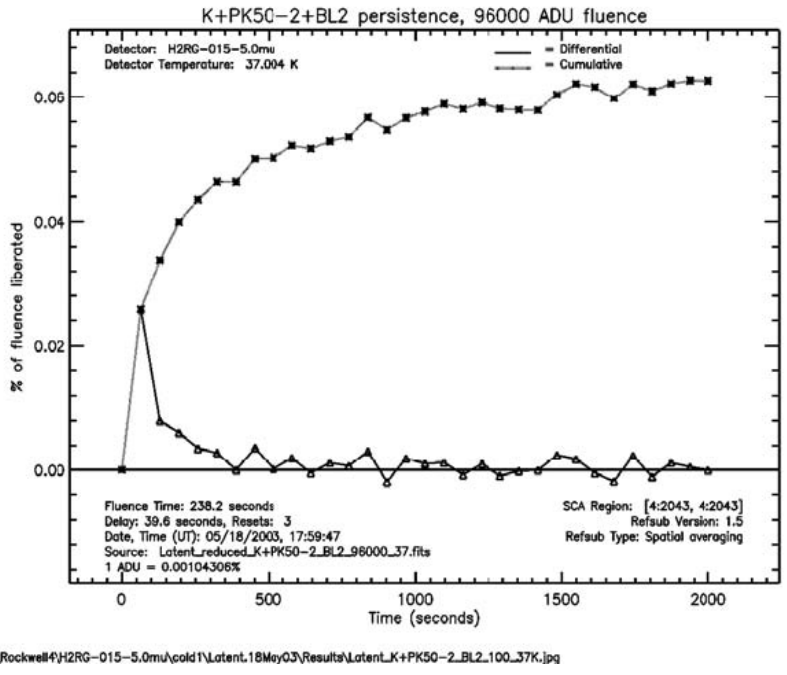

Figure 10. Latent images after ~100 percent full well capacity exposure in K-band — shows initial persistence level below 0.026%. These data are provided courtesy of Dr. Don Figer, the Independent Test Lab (IDTL) at Space Telescope and Science Institute (STScI).

For the nominal required case of ~80% full well, the initial image was ~100% of full well (100,000 ADU), and a 3 row-by-row reset sequence of the array was performed following exposure. The minimum time was slightly longer than 40 seconds before the latent image was captured due to the time limitation of moving the filter wheel. This technique, although it involves 3 resets following source exposure instead of the required 2 resets, overestimates the latent image due to excessively rapid resetting; i.e., 7 µsec per row rather than the proper 5.12 msec to match the read rate during normal data acquisition mode. Nevertheless, the first "dark" image shows only ~0.03% latent image, which drops rapidly with subsequent images. We expect better performance with the more optimized 10 µsec per pixel reset and the recommended pixel-by-pixel reset technique rather than the row-by-row reset used for the above data.

3. OVERVIEW OF THE FPA DESIGN

The FPA design concept shown in Figure 11 relies almost entirely on mechanically aligned interfaces, such as precision pins and mounting pads. This design maximizes modularity so that individual SCAs can be replaced without disturbing the neighboring SCAs. Each SCA has a dedicated electrical flex cable that passes directly out of the FPA instead of cross-connecting the SCAs inside the FPA, further enhancing modularity. This approach also minimizes the complexity associated with FPA assembly.

The relatively isothermal environment of JWST, coupled with the low electrical power dissipation of the SCA, allows the use of simple mechanical thermal joints. The use of a second interface plate (the "FPA baseplate" shown in Figure 12) provides thermal isolation to the detector plane itself so that the temperature of the detectors can be actively controlled above a slightly cooler environment. This second plate will possess all the reference surfaces for instrument mounting and represents the critical interface to the instrument for thermal, optical, mechanical, and electrical interfaces. Instrument mounting is flexible, even allowing the special case of using the instrument as the only conductive thermal interface. This option is afforded by the excellent performance of the HgCdTe detectors at warmer temperatures.

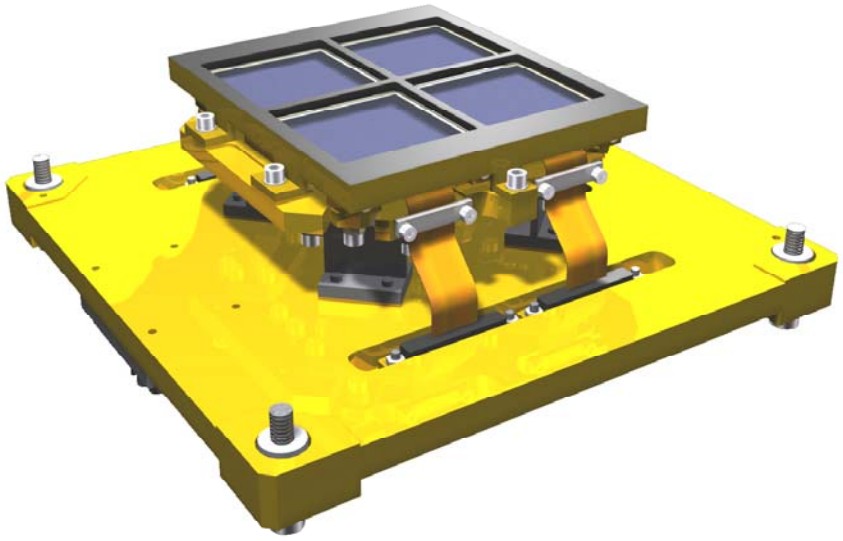

Figure 11. RSC's preliminary FPA concept — consists, from top to bottom, of a black mask over the 2x2 SCA modules, the mosaic plate under the SCAs, and thermal standoffs connecting the mosaic plate to the FPA baseplate (bottom).

A lip on one side of the molybdenum carrier base onto which the hybrid array is mounted, along the same side as the single-sided bondpads of the ROIC, allows the mounting of a multi-layer ceramic printed wirebond board (see Figure 13). Bond pads are located on the top edge of the ceramic PWB adjacent to the ROIC bond pads. The ceramic PWB extends out on this lip along the fourth (non-butted) edge of the package. It routes all of the NIRCam required hybrid ROIC bond pads to a 37-pin Kapton flex cable attached to the other edge of the PWB. The flex cable is terminated with a 37-pin micro-D connector. Surface-mount filter capacitors for the detector biases are attached to the top and bottom

side of the ceramic PWB.

The arrangement of connectors on the FPA base plate allows easy access for instrument cabling. This arrangement also permits the SCA module cable to terminate at the FPA base plate with a bulkhead mount without the need for any intermediate cable or circuit board. This enhances the modularity of the SCAs and the overall reliability of the FPA assembly.

The mosaic of SCAs is supported off the baseplate with standoffs. These standoffs provide thermal isolation and mechanical compliance between the different materials of the focal plane mosaic plate (molybdenum) and FPA baseplate (titanium) during cryogenic operation. The standoffs are sized for optimum thermal isolation and dynamic stiffness during launch.

A black mask is placed just above the detectors to block the illumination of shiny surfaces near the detector active area.

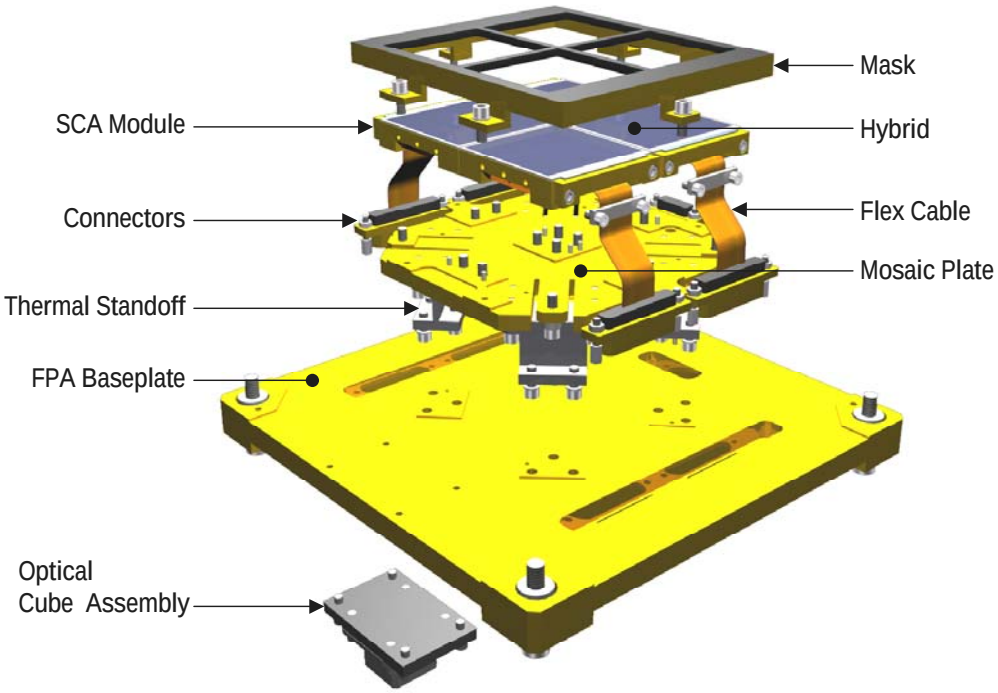

Figure 12. Exploded view of the 2x2 SCA FPA — giving a better view of the constituent parts.

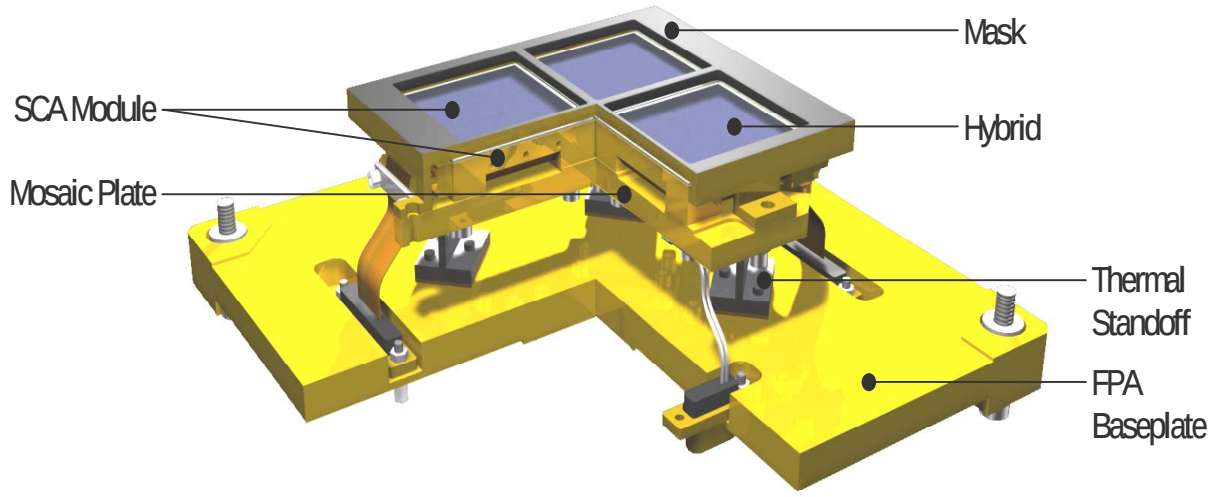

Figure 13. Cutaway view of the 2x2 SCA FPA assembly — shows the mechanical simplicity and modularity of our proposed design.

4. CONCLUSION

The science provided by the JWST mission will revolutionize astronomy, providing to astronomers of the new millennium what the Hubble Space Telescope provided to astronomers near the end of the last millennium.

Almost 6 years ago, NASA challenged the detector community to produce and demonstrate that MWIR detector arrays could achieve the ambitious performance levels required for the JWST mission. Rockwell Scientific answered the challenge in the 2000—2003 timeframe, first with the announcement that MBE HgCdTe devices had beaten the dark current and noise requirements of the mission [3]; and second, by showing this performance was repeatable in the many devices fabricated under the PMT demonstration program.

In the same timeframe, RSC fabricated 2Kx2K devices in a production environment and refined their detector growth recipe and substrate removal process to obtain high quantum efficiency devices from visible to infrared wavelengths. RSC also produced the HAWAII-2RG ROIC for the JWST mission, a premiere multiplexer for the astronomy community providing low noise and ease of operation with a tremendous amount of operational flexibility.

Rockwell Scientific, in collaboration with Ball Aerospace, is now building the NIRCam Focal Plane Assemblies and individual 2Kx2K MBE HgCdTe detector arrays to populate the flight modules. All HAWAII-2RG ROIC lot runs required for the flight program have been completed and the wafers are in-house. The detector growth and processing for both MWIR and VIS/SWIR devices have been in full production since January 2004. The first SCAs will enter the new JWST test facility in the August 2004 timeframe.

The results obtained under the precursor JWST PMT program show that the technology has demonstrated the capability of achieving the extremely difficult requirements for the JWST mission, promising to make this telescope one of the most sensitive in, or out of, this world.

ACKNOWLEDGMENTS

This work was supported by NASA Ames Research Center through contract NAS2-98077 to the University of Hawaii and Z005035 to RSC. NASA Ames Contract Technical Monitor was Dr. Craig McCreight and the University of Hawaii Principal Investigator was Dr. Donald N.B. Hall.

This paper is the result of many talented technical contributors from RSC. Thanks to M. Loose, W. E. Tennant, J.G.

Pasko, M. Carmody, C.A. Cabelli, G. Hildebrandt, J. Chow, and D.E. Cooper.

Thanks to the world-class UMC silicon foundry for fabrication of the HAWAII-2RG multiplexer.

REFERENCES

1. J.D. Garnett et al., *Performance of 5 micron, Molecular Beam Epitaxy HgCdTe Sensor Chip Assemblies (SCAs) for the NGST Mission and Ground-Based Astronomy*, Scientific Detectors for Astronomy, Kluwer Academic Publishers, Dordrecht, The Netherlands, 2004. (ISBN 1-4020-1788-X)

2. M. Loose, M.C. Farris, J.D. Garnett, D.N.B. Hall, and L.J. Kozlowski, *HAWAII-2RG: a 2k x 2k CMOS multiplexer for low and high background astronomy applications*, IR Space Telescopes and Instruments, Proceedings of SPIE, **4850** (2003), 867-879.

3. D.N.B. Hall et al., *Characterization of $\lambda c \sim 5\mu m$ Hg:Cd:Te arrays for low-background astronomy*, Optical and IR Telescope Instrumentation and Detectors, Proceedings of SPIE, **4008** (2000), 1268—1279.